nature medicine

RGMa modulates T cell responses and is involved in autoimmune encephalomyelitis

Rieko Muramatsu[1,2,8], Takekazu Kubo[3,8], Masahiro Mori[4], Yuka Nakamura[1,2], Yuki Fujita[1,2], Tsugio Akutsu[5], Tatsusada Okuno[6], Junko Taniguchi[4], Atsushi Kumanogoh[6], Mari Yoshida[7], Hideki Mochizuki[2,5], Satoshi Kuwabara[4] & Toshihide Yamashita[1–3]

In multiple sclerosis, activated CD4+ T cells initiate an immune response in the brain and spinal cord, resulting in demyelination, degeneration and progressive paralysis. Repulsive guidance molecule-a (RGMa) is an axon guidance molecule that has a role in the visual system and in neural tube closure. Our study shows that RGMa is expressed in bone marrow–derived dendritic cells (BMDCs) and that CD4+ T cells express neogenin, a receptor for RGMa. Binding of RGMa to CD4+ T cells led to activation of the small GTPase Rap1 and increased adhesion of T cells to intracellular adhesion molecule-1 (ICAM-1). Neutralizing antibodies to RGMa attenuated clinical symptoms of mouse myelin oligodendrocyte glycoprotein (MOG)-induced experimental autoimmune encephalomyelitis (EAE) and reduced invasion of inflammatory cells into the CNS. Silencing of RGMa in MOG-pulsed BMDCs reduced their capacity to induce EAE following adoptive transfer to naive C57BL/6 mice. CD4+ T cells isolated from mice treated with an RGMa-specific antibody showed diminished proliferative responses and reduced interferon-γ (IFN-γ), interleukin-2 (IL-2), IL-4 and IL-17 secretion. Incubation of PBMCs from patients with multiple sclerosis with an RGMa-specific antibody reduced proliferative responses and pro-inflammatory cytokine expression. These results demonstrate that an RGMa-specific antibody suppresses T cell responses, and suggest that RGMa could be a promising molecular target for the treatment of multiple sclerosis.

In multiple sclerosis, activated CD4+ T cells specific for components of the myelin sheath initiate an immune response in the white matter of the brain and spinal cord[1], resulting in demyelination, degeneration and progressive paralysis. Dendritic cells in the peripheral tissues and the central nervous system (CNS) are responsible for T cell activation and helper cell differentiation. T cell activation depends on the interaction of T cell receptors (TCRs) with their cognate antigen peptide presented on the surface of antigen-presenting cells (APCs), including dendritic cells and macrophages. Regulated adhesion of T cells to APCs through leukocyte function-associated antigen-1 (LFA-1) is a crucial step in the generation of a sustained TCR-mediated signal. The binding of integrins, including LFA-1, is also important for T cell trafficking into the brain[2]. The small GTPase Rap1, which is activated by antigens and chemokines, is a potent stimulator of integrins, including LFA-1 (refs. 3,4), and promotes immunological synapse formation and leukocyte migration[5].

RGMa is a membrane-bound protein that was originally identified as an axon guidance molecule in the visual system[6]. RGMa also has a role in laminar patterning in *Xenopus laevis* and chick embryos and in cephalic neural tube closure in mouse embryos[7]. Although RGMa is recognized as having a crucial role in the nervous system, we found that RGMa was expressed in dendritic cells by expression analysis in mice. This finding prompted us to investigate the role of RGMa in the immune system. This study describes a previously unknown role of RGMa in modulating T cell–mediated immune responses.

RESULTS

RGMa regulates CD4+ T cell adhesion

We first examined whether RGMa is expressed in dendritic cells. Following stimulation with lipopolysaccharide (LPS), the level of mRNA encoding RGMa was increased in the BMDCs (**Fig. 1a**). Western blot analysis confirmed that full-length RGMa (50-kDa bands) and the proteolytically cleaved mature form of RGMa (35-kDa bands) were upregulated in LPS-stimulated BDMCs (**Fig. 1b**). We then assessed whether CD4+ T cells express receptors for RGMa. Human RGMa-Fc bound to splenic CD4+ T cells in a concentration-dependent manner (**Fig. 1c**). Therefore, RGMa is induced in activated BMDCs and CD4+ T cells express receptors for RGMa.

Next, we explored the effects of RGMa on CD4+ T cell adhesion. In T lymphocytes, TCR ligation results in the transient activation of Rap1 and an increase in the GTP-bound form of Rap1 at the interface of T cells and APCs, which potentiates subsequent T cell activation[3,5]. Rap1 was activated 5 min after stimulation of splenocytes and CD4+ T cells with RGMa (**Fig. 1d**). As TCR-induced adhesion requires Rap1 activation[3,4,8], we determined whether the RGMa-induced

[1]Department of Molecular Neuroscience, Graduate School of Medicine, Osaka University, Osaka, Japan. [2]Japan Science and Technology Agency, Core Research for Evolutional Science and Technology, Tokyo, Japan. [3]Department of Neurobiology, Graduate School of Medicine, Chiba University, Chiba, Japan. [4]Department of Neurology, Graduate School of Medicine, Chiba University, Chiba, Japan. [5]Department of Neurology, Kitasato University School of Medicine, Kanagawa, Japan. [6]Department of Immunopathology, Research Institute for Microbial Diseases, Osaka University, Osaka, Japan. [7]Institute for Medical Science of Aging, Aichi Medical University, Aichi, Japan. [8]These authors contributed equally to this work. Correspondence should be addressed to T.Y. (yamashita@molneu.med.osaka-u.ac.jp).

Received 11 August 2010; accepted 2 February 2011; published online 20 March 2011; doi:10.1038/nm.2321

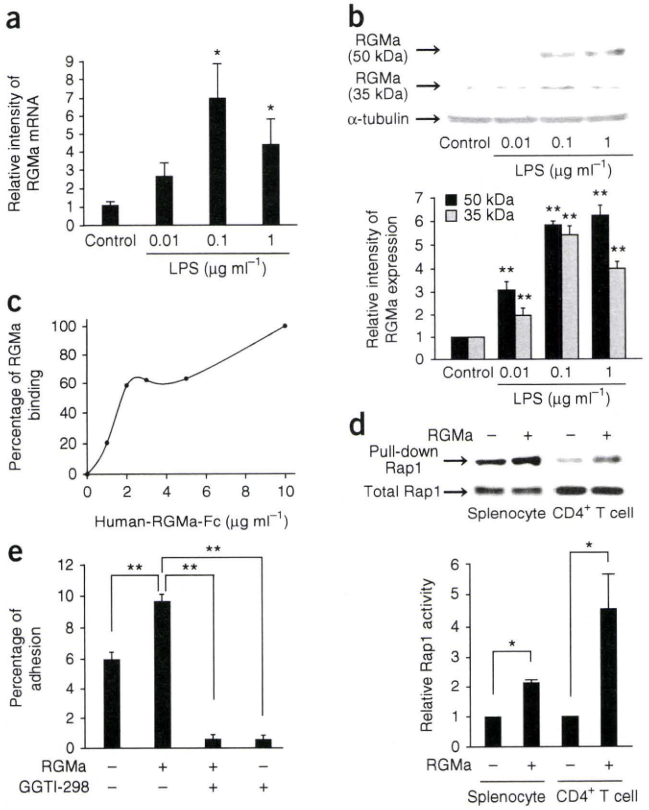

Figure 1 RGMa activates Rap1 and regulates CD4$^+$ T cell adhesion. (**a**) Quantitative RT-PCR showing relative expression level of mRNA encoding RGMa in LPS-stimulated BMDCs at the indicated concentrations for 24 h. (**b**) Western blot analysis of RGMa (50-kDa and 35-kDa bands; top rows) and α-tubulin (bottom row). Relative expression of RGMa in the BMDCs. (**c**) Binding of human RGMa-Fc to splenic CD4$^+$ T cells. (**d**) Top, representative western blot images obtained with a Rap1 pull-down assay. The bottom graph shows the relative Rap1 activity, as determined by the band intensity of RalGDS-bound Rap1 normalized to that of total Rap1 in the lysates. (**e**) CD4$^+$ T cell adhesion to ICAM-1 in the presence and absence of GGTI-298, a selective Rap1 inhibitor. Error bars are the mean ± s.e.m. of three or four independent experiments. $^*P < 0.05$ and $^{**}P < 0.01$ by one-way analysis of variance followed by Tukey's test for **a**,**b** and **e** and by Student's *t* test for **d**.

Rap1 activation alters T cell adhesion. RGMa-stimulated CD4$^+$ T cells showed stronger adhesion to ICAM-1 when compared with the control CD4$^+$ T cells (**Fig. 1e**). Moreover, a selective inhibitor of Rap1, GGTI-298, abolished RGMa-induced adhesive activity in CD4$^+$ T cells. These results suggest that RGMa enhances the adhesive activity of CD4$^+$ T cells through Rap1 activation.

Expression of RGMa and neogenin in EAE and multiple sclerosis

To assess the role of RGMa *in vivo*, we examined the expression of RGMa and neogenin, a receptor for RGMa, in the spleens, lymph nodes and spinal cord sections of C57BL/6 mice with EAE induced by MOG. Immunohistochemical analyses reveal that the majority of the CD11c$^+$ cells in these tissues expressed RGMa weakly (**Fig. 2a** and **Supplementary Fig. 1a**). RGMa expression increased in CD11c$^+$ cells after the induction of EAE (**Fig. 2a** and **Supplementary Fig. 1a**). Although RGMa was also expressed in mouse plasmacytoid dendritic cell antigen-1 (mPDCA-1)-positive cells in these tissues, its expression was unchanged after the induction of EAE (**Fig. 2b** and **Supplementary Fig. 1b**). Furthermore, CD4$^+$ T cells in these tissues expressed neogenin. Expression of neogenin did not change during the observation period after the induction of EAE (**Fig. 2c** and **Supplementary Fig. 1c**). Next, we assessed Rap1 activity *in situ* to determine whether Rap1 is activated in CD4$^+$ T cells in the CNS after induction of EAE. Activated Rap1 was present in CD4$^+$ T cells in the cervical spinal cords of EAE mice but not in control mice (**Fig. 2d**).

We performed immunohistochemical analyses on autopsied samples of brain and spinal cord obtained from eight individuals with multiple sclerosis. We evaluated the presence of mature and immature dendritic cells in these tissues by using antibodies to CD83 and CD209 (also known as DC-SIGN), respectively[9]. CD83$^+$ and CD209$^+$ dendritic cells were immunoreactive for RGMa in the brain and spinal cord sections of individuals with multiple sclerosis (**Fig. 2e**), but not in sections from control brains (data not shown). To examine the expression of neogenin in human cells, we purified peripheral blood mononuclear cells (PBMCs) from individuals with relapsing-remitting multiple sclerosis. CD3$^+$ T cells from these samples expressed neogenin at the time of relapse and during the remission phase (**Fig. 2f**). Neogenin expression did not differ in PBMCs from individuals with multiple sclerosis or healthy controls (**Fig. 2g**). Furthermore, neogenin was expressed in CD3$^+$ T cells in brain and spinal cord sections from individuals with multiple sclerosis (**Supplementary Fig. 1d**).

RGMa-specific antibodies attenuate clinical signs in EAE

To determine whether RGMa inhibition alters the clinical severity of EAE, we intraperitoneally administered RGMa-specific antibodies[10] or control rabbit IgGs to mice on days 7 and 10 after immunization with MOG. The antibody was detectable in the spleen and lymph nodes at day 7 after administration (**Supplementary Fig. 2a**). RGMa-specific antibody treatment reduced the clinical severity of the disease (**Fig. 3a**) and the percentage of mice that presented with clinical signs of EAE (**Fig. 3b**), but did not delay the day of onset of EAE clinical symptoms (**Fig. 3c**). However, the mean maximum EAE score (**Fig. 3d**) and the cumulative EAE scores (**Fig. 3e**) were lower in RGMa-specific antibody–treated mice as compared with control IgG–treated mice. These data show that RGMa-specific antibody treatment attenuates the severity of EAE.

RGMa-specific antibody treatment reduced the infiltration of cells in the spinal cord at day 21 after the induction of EAE in mice (**Fig. 3f,g**). The accumulation of CD4$^+$, CD11b$^+$, F4/80$^+$, B220$^+$, CD11c$^+$ and mPDCA-1$^+$ cells in the spinal cord (**Fig. 3h**) of EAE mice decreased as a result of treatment with the RGMa-specific antibody. Myelin loss and axonal damage in EAE mice was also reduced following treatment with the RGMa-specific antibody (**Fig. 3i,j**) Thus, RGMa-specific antibody treatment reduces inflammatory cell accumulation and histological damage following the induction of EAE.

A role for RGMa in T cell activation in EAE

To confirm whether RGMa expressed on dendritic cells modulates EAE, we carried out adoptive transfer experiments with MOG-pulsed BMDCs following RGMa knockdown. Transfection of BMDCs with RGMa siRNA downregulated RGMa expression (**Supplementary Fig. 2b**). Recipient C57BL/6 mice injected intravenously with RGMa siRNA-transfected, MOG-pulsed BMDCs had moderately reduced clinical disease scores as compared with mice injected with control siRNA–transfected, MOG-pulsed BMDCs

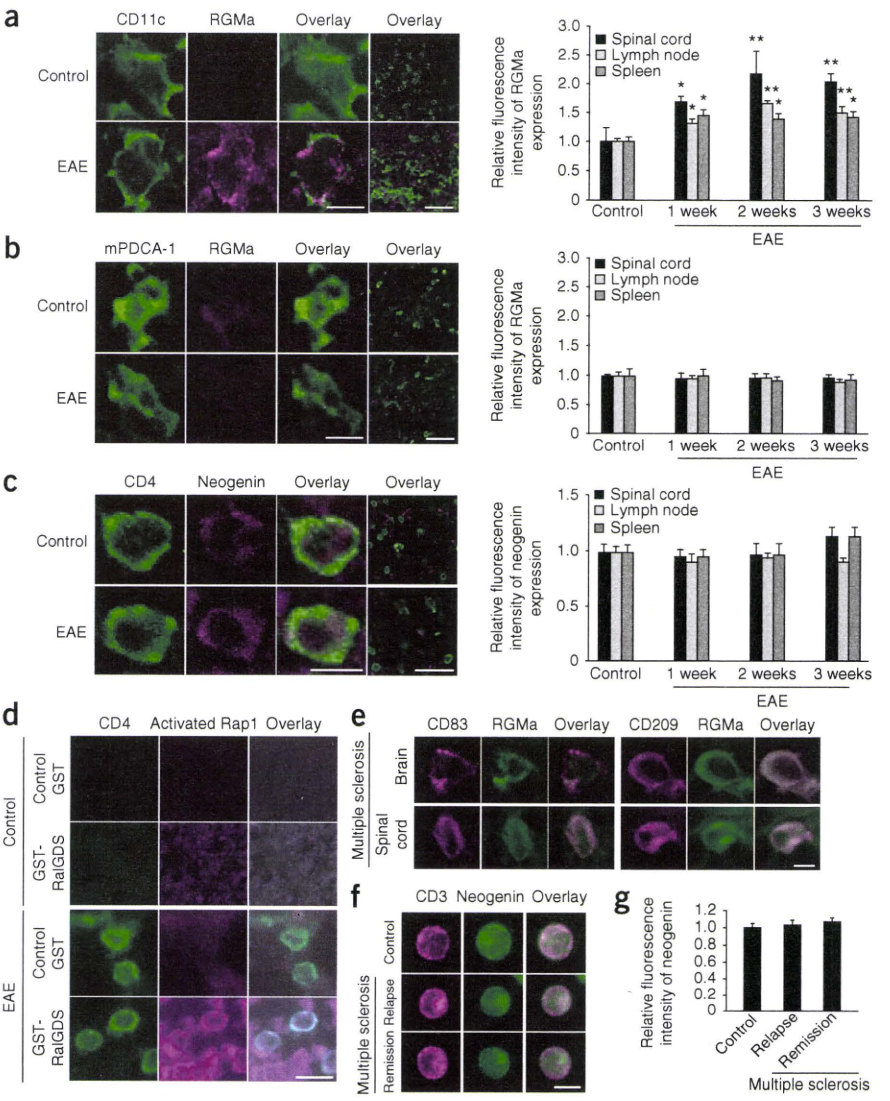

Figure 2 Expression of RGMa and neogenin in MOG-induced EAE and multiple sclerosis tissue. (**a**) Frozen sections of the spleen immunostained for RGMa (labeled with Alexa Fluor 568) and CD11c (labeled with Alexa Fluor 488) in EAE and control mice. The graph shows the relative expression of RGMa in $CD11c^+$ cells in the lymph node, spleen and spinal cord before (control) and 1, 2 and 3 weeks after immunization with MOG. $n = 37–51$ cells for each mouse. $^*P < 0.05$ and $^{**}P < 0.01$ by one-way analysis of variance followed by Tukey's test. (**b**) The sections (same sections as shown in **a**) of the spleen immunostained for RGMa (labeled with Alexa Fluor 568) and plasmacytoid dendritic cells (mPDCA-1) (labeled with Alexa Fluor 488). The graph shows the relative expression of RGMa in mPDCA-1^+ cells. $n = 40–48$ cells for each mouse. (**c**) Expression of neogenin (labeled with Alexa Fluor 568) in $CD4^+$ T cells (labeled with Alexa Fluor 488) in the spleen. The graph shows the relative expression of neogenin in $CD4^+$ T cells. (**d**) *In situ* Rap1 pull-down assay (labeled with Alexa Fluor 568) in $CD4^+$ T cells (labeled with Alexa Fluor 488) in cervical spinal cord tissue sections of EAE and control mice. (**e**) Multiple sclerosis brain and spinal cord tissues sections double-labeled for RGMa (with Alexa Fluor 488) in combination with CD83 or CD209 (DC-SIGN) (labeled with Alexa Fluor 568) $n = 8$. (**f**) Expression of neogenin (labeled with Alexa Fluor 488) in human $CD3^+$ cells (labeled with Alexa Fluor 568) in relapsing-remitting multiple sclerosis and healthy control PBMCs. (**g**) Relative fluorescence intensity of neogenin in the immunohistochemical analysis. Error bars represent the mean ± s.e.m. of 3 or 4 independent experiments. Scale bars in **a**–**e**, 50 μm for low (overlay images in **a**, **b**, and **c**) and 10 μm for high (all other images) magnification images; scale bar in **f**, 5 μm.

(**Fig. 4a**). The adoptive transfer of RGMa siRNA–transfected BMDCs resulted in reduced $F4/80^+$ cell infiltration into the spinal cord at day 21 after EAE induction (**Supplementary Fig. 2c**).

To further address whether dendritic cell–derived RGMa has a role in T cell activation, we immunized C57BL/6 mice with MOG, followed by treatment with RGMa-specific antibodies or control antibodies at days −2, 0 and 5 after immunization. On day 10 after immunization, we collected cells from the spleen and draining lymph nodes of the treated mice, re-stimulated these cells with MOG peptide, purified $CD4^+$ T cells from these cells and then adoptively transferred them into naïve recipient mice. The EAE clinical scores (see **Supplementary Methods**) were moderately reduced in C57BL/6 mice that were injected with $CD4^+$ T cells from RGMa-specific antibody–treated EAE mice as compared with mice injected with $CD4^+$ T cells from the IgG control antibody–treated mice (**Fig. 4b**).

Next, we assessed whether the RGMa-specific antibody directly inhibits T cell trafficking to the CNS. We immunized transgenic mice that ubiquitously express EGFP (CAG-EGFP mice) with MOG, isolated splenocytes from these mice 7 d after immunization and re-stimulated splenocytes with MOG for 3 d. We treated naïve recipient C57BL/6 mice with control IgG or RGMa-specific antibody 3 d before and at the time of transfer of the re-stimulated $CD4^+$ T cells. At day 10 after adoptive transfer, there was no significant difference in the infiltration of EGFP-labeled T cells into the CNS of control or RGMa-specific antibody–treated mice (**Fig. 4c**). Consistent with these *in vivo* observations, the RGMa-specific antibody did not inhibit adhesion of splenic $CD4^+$ T cells from EAE mice to ICAM-1 *in vitro* (**Fig. 4d**). This result excludes the possibility that the antibody directly interfered with the adhesion of $CD4^+$ T cells to ICAM-1. Furthermore, using an *in vitro* model of the blood-brain barrier consisting of brain-derived capillary endothelial b-End3 cells, splenic $CD4^+$ T cells from MOG-EAE mice transmigrated more readily across the b-End3 cells than did $CD4^+$ T cells isolated from EAE mice treated (*in vivo*) with the RGMa-specific antibody (**Fig. 4e**). However, transmigration of T cells was not altered following direct addition of RGMa-specific antibody *in vitro* to splenic $CD4^+$ T cells (**Fig. 4e**). Because Rap1 activity is associated with increased adhesion of T cells, we measured Rap1 activity by pull-down assay and found that Rap1 activity was reduced in $CD4^+$ T cells isolated from EAE-mice treated with the RGMa-specific antibody (**Fig. 4f**). However, we did not observe marked suppression of Rap1 activity following *in vitro* treatment of $CD4^+$ T cells with the RGMa-specific antibody (**Fig. 4f**). Thus, we obtained no evidence suggesting that the RGMa-specific antibody directly modulates the trafficking of T cells to the CNS.

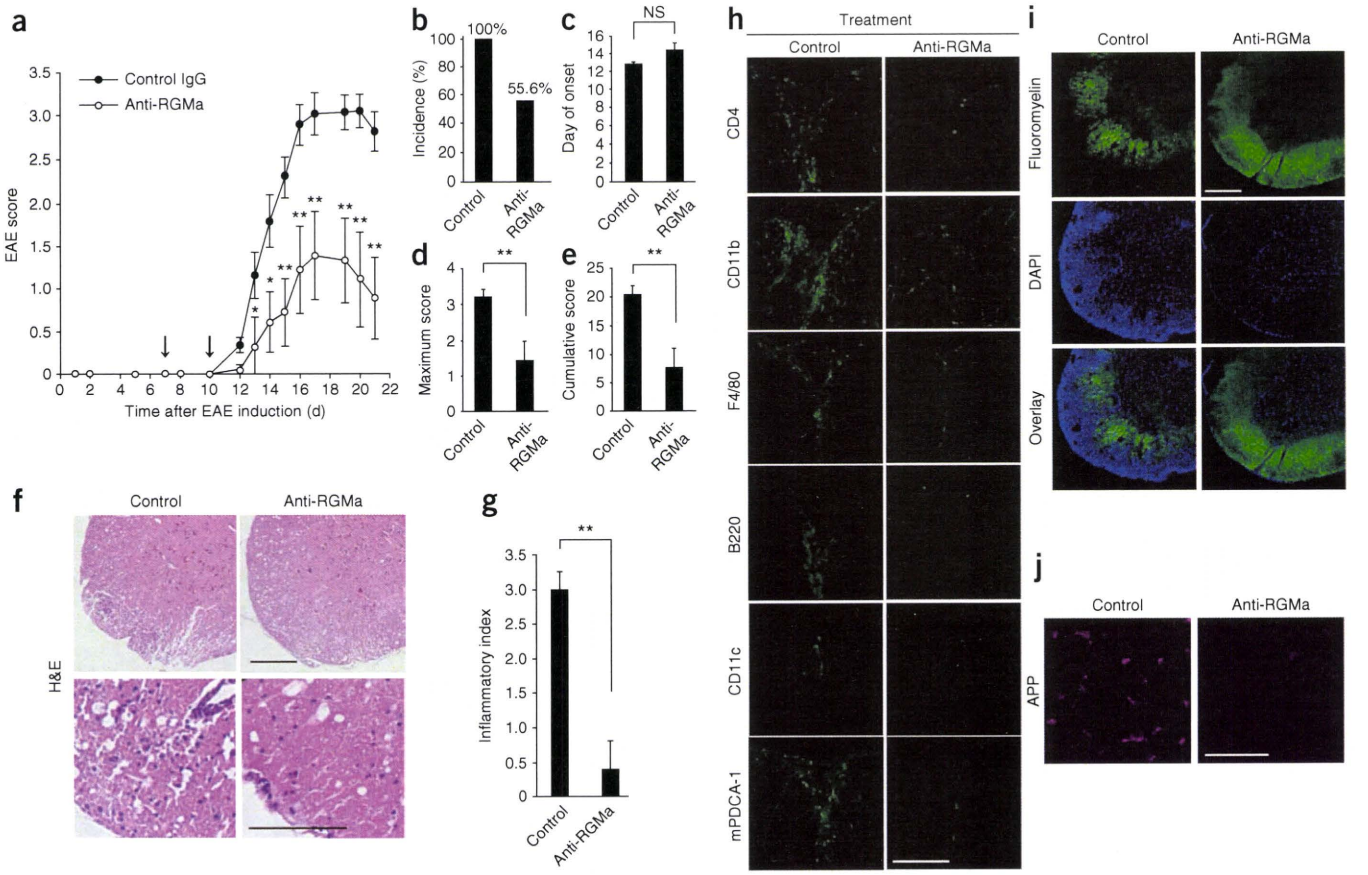

Figure 3 RGMa-specific antibody treatment reduces the severity of MOG-induced EAE. (**a**) Clinical EAE disease scores (EAE score) in mice treated with control IgGs ($n = 16$) and RGMa-specific antibodies (anti-RGMa; $n = 9$). Data represent the mean ± s.e.m. $^*P < 0.05$, and $^{**}P < 0.01$ by Mann-Whitney's U test. The arrows represent the time points of antibody administration. (**b**) Incidence of EAE clinical signs in MOG-induced EAE mice treated with control IgGs or RGMa-specific antibodies. (**c**) The average day of disease onset between the two treatment groups. (**d**) The mean ± s.e.m. of the maximum EAE score of each mouse with EAE. (**e**) The mean ± s.e.m. of the cumulative EAE scores. $^*P < 0.05$ and $^{**}P < 0.01$ by Student's t test. NS, not significant. (**f**) H&E staining of the cervical spinal cord in RGMa-specific antibody– and control IgG–treated mice. (**g**) Histological scores (inflammatory index; see **Supplementary Methods**) for the inflammatory lesions. Error bars represent the mean ± s.e.m. (control IgG, $n = 6$; RGMa-specific antibody, $n = 5$). $^*P < 0.01$ by Student's t test. (**h**) Representative images of $CD4^+$, $CD11b^+$, $F4/80^+$, $B220^+$, $CD11c^+$ and $mPDCA\text{-}1^+$ cells in the spinal cord of control IgG- and RGMa-specific antibody–treated EAE mice. (**i**,**j**) FluoroMyelin (**i**) and APP (**j**) staining in the spinal cord of IgG- and RGMa-specific antibody–treated mice. Scale bars in **f**,**h**,**i**, 200 μm; scale bar in **j**, 100 μm.

In contrast to MOG, which causes chronic EAE, proteolipid protein $(PLP)_{139-151}$ peptide induces relapsing-remitting EAE in SJL/J mice, which depends on continued activation of T cells via endogenous myelin epitopes (epitope spreading)[11]. We intraperitoneally administered the RGMa-specific antibody or control rabbit IgG to mice on days 25 and 28 after immunization with $PLP_{139-151}$. These time points correspond to the late stage of the first paralytic incident (a clinical feature of EAE). Treatment with the RGMa-specific antibody was moderately effective in reducing the clinical severity of relapses (**Fig. 4g**). Furthermore, it is known that T cell activation due to epitope spreading occurs directly in the CNS[12]. Indeed, we detected the presence of the RGMa-specific antibody in sections of the brain and the spinal cord after intraperitoneal administration (**Supplementary Fig. 2d**), suggesting the RGMa-specific antibody inhibits the activation of T cells by local APCs, possibly dendritic cells, in the CNS.

The role of RGMa in macrophages and microglia

Next, we performed additional experiments to characterize the effects of RGMa in other cell types. Macrophages expressed neogenin (**Supplementary Fig. 3a**,**b**) but not RGMa (**Supplementary Fig. 3c**,**d**), whereas microglia express RGMa (ref. 10). In B cells, B220 and RGMa did not colocalize in spinal cord sections of MOG-EAE mice (**Supplementary Fig. 3c**).

To assess whether the neogenin expressed in macrophages plays a role in EAE, we used CD11b-DTR mice in which macrophages can be selectively depleted[13]. To specifically knockdown neogenin in macrophages, we adoptively transferred macrophages with or without neogenin knockdown (**Supplementary Fig. 3e**) into CD11b-DTR mice after depletion of host macrophages. EAE was then induced via MOG immunization in the recipient mice. The clinical severity of the disease did not differ between the recipient mice with wild-type macrophages or macrophage-specific neogenin knockdown (**Supplementary Fig. 4a**). Next, we attempted to inhibit the RGM-neogenin signals in microglia in the CNS by delivering the RGMa-specific antibody or control IgG intrathecally. The clinical severity of the resultant MOG-induced EAE did not differ between the two mouse groups (**Supplementary Fig. 4b**). Thus, RGM-neogenin signals in macrophages and microglia do not appear to contribute significantly to the clinical course of EAE.

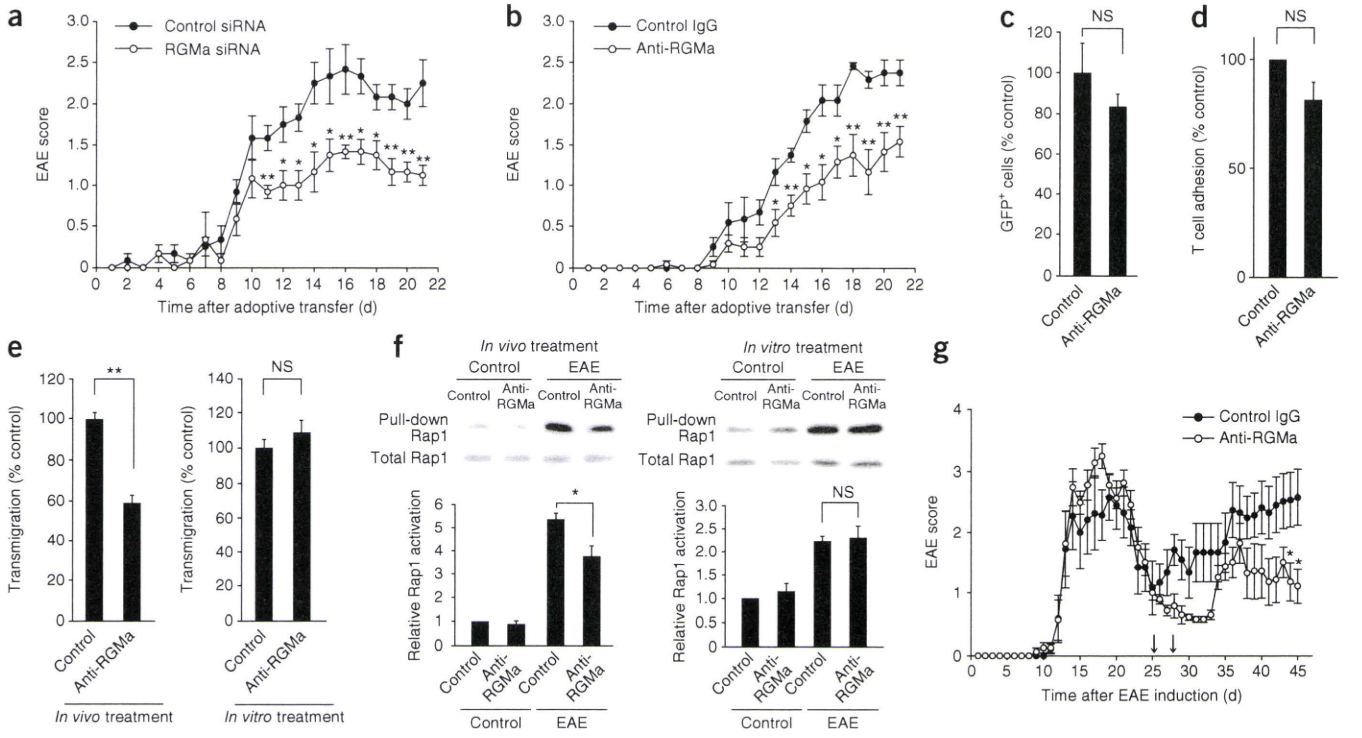

Figure 4 RGMa-specific antibody treatment suppresses T cell responses in EAE. (**a**) EAE scores in mice after adoptive transfer of MOG-stimulated BMDCs with or without RGMa knockdown. (**b**) EAE scores in mice after adoptive transfer of re-stimulated CD4$^+$ T cells from donor mice immunized with MOG with or without the RGMa-specific antibody treatment (anti-RGMa). (**c**) Number of GFP-labeled CD4$^+$ T cells in the brain sections of control recipient mice and mice treated with RGMa-specific antibody at day 10 after adoptive transfer of the re-stimulated EGFP-labeled CD4$^+$ T cells. (**d**) Percentage of CD4$^+$ T cells obtained from MOG-EAE mice that adhered to ICAM-1 in the presence of RGMa-specific or control antibodies *in vitro*. (**e**) Transmigration of CD4$^+$ T cells across b-End3 cells. Left, CD4$^+$ T cells from EAE mice treated *in vivo* with control IgG or RGMa-specific antibody; right, CD4$^+$ T cells from EAE mice treated *in vitro* with control IgG or RGMa-specific antibody. (**f**) Top, representative western blots obtained by Rap1 pull-down assay. Bottom, relative Rap1 activity. (**g**) EAE scores after intraperitoneal injection of RGMa-specific antibody or control IgG in SJL/J mice immunized with PLP. Number of mice in each group: control siRNA: 5, RGMa siRNA: 5 (**a**); control IgG: 7, RGMa-specific antibody: 7 (**b**); control IgG: 5, RGMa-specific antibody: 5 (**c**); control IgG: 4, RGMa-specific antibody: 4 (**d**), each group: 4 (**e**); each group: 3 (**f**); and control IgG: 11, RGMa-specific antibody: 9 (**g**). Error bars in all panels represent the means ± s.e.m; $*P < 0.05$ and $**P < 0.01$ as compared with control group by Mann-Whitney's *U* test for **a**,**b** and **g** and Student's *t* test for **c**–**f**.

Finally, to assess whether the effect of the RGMa-specific antibody on the peripheral immune system is specific to autoimmune CNS inflammation, we used a spinal cord injury (SCI) mouse model, as SCI elicits nonautoimmune CNS inflammation. We intraperitoneally administered the RGMa-specific antibody at 0 and 3 d after SCI. Intraperitoneal administration of the RGMa-specific antibody did not substantially enhance the recovery of locomotor activity after SCI (**Supplementary Fig. 4c**). Therefore, the results suggest that the effect of the RGMa-specific antibody is specific to autoimmune CNS inflammation.

RGMa-specific antibodies regulate T cell responses

Next, we sought to investigate whether RGMa-specific antibody treatment inhibits T cell activation and cytokine release. Splenocytes from MOG-immunized mice treated with RGMa-specific or control antibodies were isolated at day 21 after EAE induction and re-stimulated *in vitro* with the MOG peptide or with CD3-specific antibodies. RGMa-specific antibody treatment diminished the MOG-specific T cell proliferative response (**Fig. 5a**), reduced IL-2, IL-4, IFN-γ and IL-17 secretion and increased IL-10 secretion (**Fig. 5a**). We observed similar effects of RGMa-specific antibody treatment on the T cell proliferative response and cytokine secretion following *in vitro* simulation with CD3-specific antibodies (**Supplementary Fig. 5a–c**).

Finally, we examined T cell proliferation and cytokine production by PBMCs isolated from 17 individuals with relapsing-remitting multiple sclerosis (eight during relapse and nine in the remission phase). RGMa-specific antibody treatment decreased the phorbol 12-myristate 13-acetate (PMA) plus ionomycin–induced T cell proliferative responses (**Fig. 5b**). PBMCs from individuals with clinically relapsing multiple sclerosis also expressed mRNA encoding IL-2, IL-4, IFN-γ and IL-17 following stimulation with PMA plus ionomycin (**Fig. 5b**). Addition of the RGMa-specific antibody reduced expression of these cytokine mRNAs, but did not affect cytokine expression in PBMCs that were not incubated with PMA plus ionomycin (**Fig. 5b**). The level of mRNA encoding IL-10 was increased in T cells incubated with PMA plus ionomycin and the RGMa-specific antibody (**Fig. 5b**). We obtained similar results in the PBMCs obtained from individuals with multiple sclerosis in the remission phase, although the effect of the RGMa-specific antibody on cytokine expression was attenuated (**Fig. 5b**). Therefore, the RGMa-specific antibody modulates T cell proliferative responses and cytokine expression in PBMCs from individuals with multiple sclerosis.

DISCUSSION

Treatment with the RGMa-specific antibody effectively suppresses T cell responses and attenuates the clinical course of EAE. Results obtained

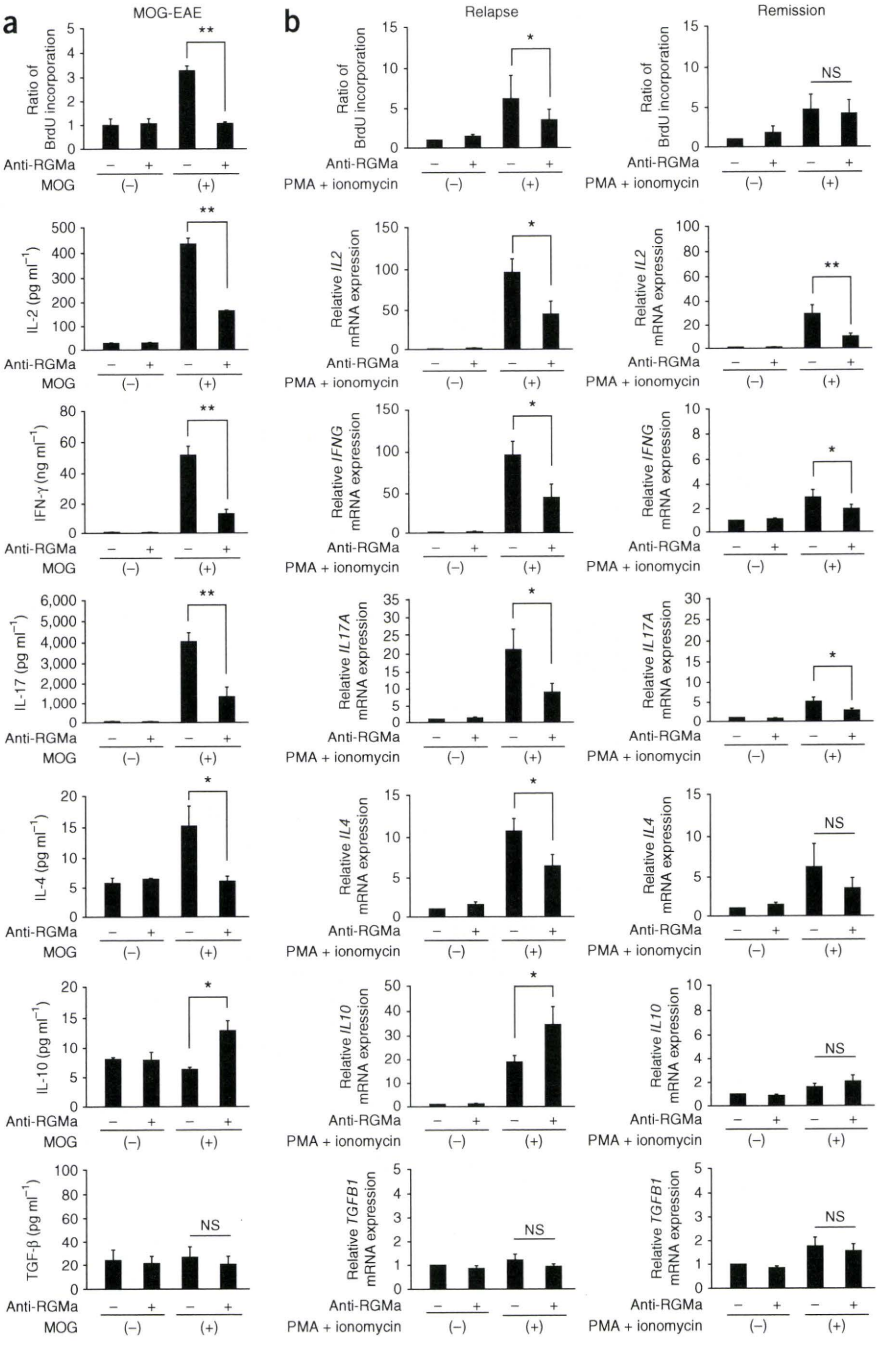

Figure 5 T cell proliferation and cytokine production from MOG-EAE mice and PBMCs from humans with multiple sclerosis. (**a**) Top graph, MOG-specific proliferative responses in splenic cells obtained from mice treated with RGMa-specific antibody (anti-RGMa) or control IgG at d 21 after MOG immunization. Each bar represents the mean ± s.e.m. (control IgG, $n = 6$; RGMa-specific antibody, $n = 5$). Bottom graphs, production of IL-2, IFN-γ, IL-17, IL-4, IL-10 and TGF-β by spleen cells obtained from mice treated with RGMa-specific antibody or control IgGs. Each bar represents the mean ± s.e.m. (control IgG, $n = 6$; RGMa-specific antibody, $n = 5$). $^*P < 0.05$, and $^{**}P < 0.01$ by Student's *t*-test. (**b**) Relative levels of cell proliferation (top two graphs) and relative levels of cytokine mRNA (bottom graphs) from PBMCs stimulated with PMA plus ionomycin in the presence or absence of the RGMa-specific antibody. PBMCs were obtained from individuals with relapsing-remitting multiple sclerosis (8 in clinical relapse; 9 in clinical remission). Each error bar represents the mean ± s.e.m; $^*P < 0.05$ and $^{**}P < 0.01$ by Student's *t* test.

by adoptive transfer experiments suggest that RGMa expressed in dendritic cells activates T cells in the peripheral tissues. However, RGMa-specific antibody also reduces the severity of relapses in PLP-induced EAE, suggesting that the RGMa-specific antibody may inhibit T cell activation by APCs in the CNS as well.

As RGMa-specific antibodies suppress the T cell responses induced by antibody to CD3 *in vitro*, it may provide a global immunosuppression strategy. However, as we did not observe an improvement in locomotor recovery after SCI following the intraperitoneal injection of the RGMa-specific antibody, the immunomodulatory effect of the antibody in SCI remains unexplained. Our results in PBMCs from patients with multiple sclerosis suggest that inhibition of RGMa reduces T cell proliferation and cytokine release. Notably, RGMa polymorphisms are associated with multiple sclerosis and correlate with the changes in IFN-γ and tumor necrosis factor expression in the cerebrospinal fluid of individuals with multiple sclerosis[14].

The role of RGMa in limiting repair of the neural network should also be considered. Axonal damage is both an early event in the development of lesions in multiple sclerosis[15] and EAE[16] and a major determinant of clinical disability. Repair of the axonal damage induced by EAE is facilitated by selectively inhibiting the activities of Nogo-A, a myelin-derived inhibitor of axon growth[17]. Knockdown or inhibition of leucine-rich repeat and Ig domain–containing-1 (LINGO-1), a negative regulator of axonal myelination, promotes functional recovery in EAE[18]. Promoting the restoration of the injured neural network could also account for some of the beneficial effects of the RGMa-specific antibody. Future studies will be aimed at elucidating what targets of the RGMa-specific antibody are necessary for the beneficial effects on EAE. Taken together, our findings suggest that RGMa may prove to be a promising molecular target for the treatment of multiple sclerosis.

METHODS

Methods and any associated references are available in the online version of the paper at http://www.nature.com/naturemedicine/.

Note: Supplementary information is available on the Nature Medicine website.

ACKNOWLEDGMENTS

This work was supported by a Grant-in-Aid for Young Scientists (S) from the Japan Society for the Promotion of Sciences (19679007) to T.Y., and a Grant-in-Aid from Ministry of Health, Labour and Welfare to T.Y. We thank H. Hayakawa and members of the Yamashita laboratory for fruitful discussion and help.

AUTHOR CONTRIBUTIONS
T.K. performed preliminary experiments for expression analysis, behavioral and histological analysis of EAE, and cytokine production, and contributed to conceiving the study. Later, R.M. took over the work and performed all experiments, with the exception of the portions indicated below. Y.N. performed EAE induction, adoptive transfer experiments, immunohistochemical analyses and spinal cord injury experiments. Y.F. performed the lymphocyte binding assay, Rap1 activity assay and cytokine analysis. M.M., J.T. and S.K. performed experiments with PBMCs. T.O. helped with irradiation experiments. M.M., T.A., J.T., M.Y., H.M. and S.K. performed experiments with autopsy samples. T.K and T.Y. conceived the project and developed the hypothesis. T.K, R.M., A.K. and T.Y. designed the experiments. A.K. and T.O. discussed the hypothesis and helped with data interpretation. T.Y. coordinated and directed the project and wrote the manuscript.

COMPETING FINANCIAL INTERESTS
The authors declare no competing financial interests.

Published online at http://www.nature.com/naturemedicine/.
Reprints and permissions information is available online at http://npg.nature.com/reprintsandpermissions/.

1. Trapp, B.D., Ransohoff, R.M., Fisher, E. & Rudick, R. Neurodegeneration in multiple sclerosis: relationship to neurological disability. *Neuroscientist* **5**, 48–57 (1999).
2. Smith, A. *et al.* The role of the integrin LFA-1 in T-lymphocyte migration. *Immunol. Rev.* **218**, 135–146 (2007).
3. Katagiri, K. *et al.* Rap1 is a potent activation signal for leukocyte function-associated antigen 1 distinct from protein kinase C and phosphatidylinositol-3-OH kinase. *Mol. Cell. Biol.* **20**, 1956–1969 (2000).
4. Reedquist, K.A. *et al.* The small GTPase, Rap1, mediates CD31-induced integrin adhesion. *J. Cell Biol.* **148**, 1151–1158 (2000).
5. Katagiri, K., Hattori, M., Minato, N. & Kinashi, T. Rap1 functions as a key regulator of T-cell and antigen-presenting cell interactions and modulates T-cell responses. *Mol. Cell. Biol.* **22**, 1001–1015 (2002).
6. Stahl, B., Müller, B., von Boxberg, Y., Cox, E.C. & Bonhoeffer, F. Biochemical characterization of a putative axonal guidance molecule of the chick visual system. *Neuron* **5**, 735–743 (1990).
7. Yamashita, T., Mueller, B.K. & Hata, K. Neogenin and repulsive guidance molecule signaling in the central nervous system. *Curr. Opin. Neurobiol.* **17**, 29–34 (2007).
8. Suga, K. *et al.* CD98 induces LFA-1–mediated cell adhesion in lymphoid cells via activation of Rap1. *FEBS Lett.* **489**, 249–253 (2001).
9. Serafini, B. *et al.* Dendritic cells in multiple sclerosis lesions: maturation stage, myelin uptake and interaction with proliferating T cells. *J. Neuropathol. Exp. Neurol.* **65**, 124–141 (2006).
10. Hata, K. *et al.* RGMa inhibition promotes axonal growth and recovery after spinal cord injury. *J. Cell Biol.* **173**, 47–58 (2006).
11. McRae, B.L., Vanderlugt, C.L., Dal Canto, M.C. & Miller, S.D. Functional evidence for epitope spreading in the relapsing pathology of experimental autoimmune encephalomyelitis. *J. Exp. Med.* **182**, 75–85 (1995).
12. McMahon, E.J. *et al.* Epitope spreading initiates in the CNS in two mouse models of multiple sclerosis. *Nat. Med.* **11**, 335–339 (2005).
13. Duffield, J.S. *et al.* Selective depletion of macrophages reveals distinct, opposing roles during liver injury and repair. *J. Clin. Invest.* **115**, 56–65 (2005).
14. Nohra, R. *et al.* RGMA and IL21R show association with experimental inflammation and multiple sclerosis. *Genes Immun.* **11**, 279–293 (2010).
15. Trapp, B.D., Ransohoff, R. & Rudick, R. Axonal pathology in multiple sclerosis: relationship to neurologic disability. *Curr. Opin. Neurol.* **12**, 295–302 (1999).
16. Onuki, M., Ayers, M.M., Bernard, C.C. & Orian, J.M. Axonal degeneration is an early pathological feature in autoimmune-mediated demyelination in mice. *Microsc. Res. Tech.* **52**, 731–739 (2001).
17. Karnezis, T. *et al.* The neurite outgrowth inhibitor Nogo A is involved in autoimmune-mediated demyelination. *Nat. Neurosci.* **7**, 736–744 (2004).
18. Mi, S. *et al.* LINGO-1 antagonist promotes spinal cord remyelination and axonal integrity in MOG-induced experimental autoimmune encephalomyelitis. *Nat. Med.* **13**, 1228–1233 (2007).

ONLINE METHODS

Mice. C57BL/6 (Japan SLC), SJL/J (Charles River), CAG-EGFP (Japan SLC) mice and CD11b-DTR mice (The Jackson Laboratory) (ages: 8–10 weeks; C57BL/6, SJL/J, and CAG-EGFP mice: male; CD11b-DTR mice: 7 male and 3 female) were bred and maintained. The Institutional Animal Care and Use Committees of Graduate School of Medicine, Chiba University and Osaka University approved all experimental procedures.

EAE induction. We induced EAE by subcutaneous injection of 200 μl of an emulsion (1:1 PBS or complete Freund's adjuvant (CFA, Difco) containing 100 μg of MOG_{35-55} peptide (MEVGWYRSPFSRVVHLYRNGK) (Greiner Bio-One) to C57BL/6 mice or $PLP_{139-151}$ peptide (HSLGKWLGHPDKF) (Greiner Bio-One) to SJL/J mice in PBS and 500 μg of *Mycobacterium tuberculosis* extract H37Ra (Difco) in CFA. At 0 h and 48 h after immunization, mice received 200 ng of pertussis toxin intravenously (List Biological Laboratories). 400 μg of RGMa-specific antibodies (28045F; IBL) or control antibodies (rabbit IgG; I5006; Sigma-Aldrich) were administered intraperitoneally to mice on days 7 and 10 after MOG immunization and on day 25 and 28 after PLP immunization. We generated RGMa-specific rabbit antisera against the synthetic peptide (residues 309–322) as the immunogen. The peptide sequence is specific to RGMa but has no similarity to the RGMb or RGMc sequence. The antisera were purified by affinity chromatography. The antibody blocked the inhibitory effect of RGMa on neurite growth[10].

Adoptive transfer experiments. For adoptive transfer of BMDCs with RGMa knockdown, we intravenously injected mice with 6×10^5 cells per 0.1 ml live BMDCs pulsed *in vitro* with 100 μg ml^{-1} MOG_{35-55} for 4–6 h. We subcutaneously injected mice with 0.2 ml of CFA containing 500 μg of *Mycobacterium tuberculosis*. Mice received 200 ng of pertussis toxin intravenously 0 h and 48 h after immunization.

We also immunized donor mice with MOG in CFA with or without the RGMa-specific antibody treatment (days −2, 0 and 5). On day 10 after immunization, we collected the spleens and draining lymph nodes, prepared single-cell suspensions and lysed red blood cells. Cells (5×10^6 cells per ml) were cultured with 40 μg ml^{-1} MOG_{35-55} peptide. After 3 d of culture, we collected cells and isolated $CD4^+$ T cells by negative selection with a $CD4^+$ T cell isolation kit (Miltenyi Biotec). Sublethally irradiated (500 Gy) mice intravenously received the cells.

T cell proliferation and cytokine analysis. On day 21 after induction of EAE, we cultured splenocytes (5×10^5 cells per 0.1 ml) from these mice with in 96-well plates in RPMI-1640 medium supplemented with glutamine (Gibco), sodium pyruvate (Gibco), penicillin (Gibco), streptomycin (Gibco), 2-ME (Wako) and 10% (vol/vol) heat-inactivated FBS (Gibco) for the proliferation assay. $CD4^+$ T cells were re-stimulated with 20 μg ml^{-1} of MOG peptide or 5 μg ml^{-1} of CD3-specific monoclonal antibody (2C11; BD Biosciences). We estimated cell proliferation by measuring BrdU incorporation into the newly synthesized cellular DNA for 24 h with a cell proliferation enzyme-linked immunosorbent assay and BrdU (colorimetric) assay (Roche Diagnostics) according to the manufacturer's instructions. To measure the production of IL-2, IFN-γ, IL-17, IL-4, IL-10 and TGF-β, we cultured the splenocytes (2×10^6 cells per ml) obtained from the mice with EAE in 24-well plates with or without 20 μg ml^{-1} of MOG peptide or 5 μg ml^{-1} of the CD3-specific monoclonal antibody. We collected the supernatants after 72 h in culture. We then performed cytokine ELISAs according to the manufacturer's instructions (IL-2, IFN-γ, IL-17, IL-4: BioSource, Invitrogen; IL-10 and TGF-β, R&D Systems).

Human subjects. The research protocol was approved by the Human Use Review Committees of the Graduate School of Medicine, Chiba University; Kitasato University School of Medicine; and Aichi Medical University. Informed consent was obtained from all subjects. 17 individuals with relapsing-remitting multiple sclerosis were diagnosed according to the McDonald criteria[19]. We obtained samples from eight individuals (seven women; median age: 39.0 years; range: 24–57 years) during clinical relapse and nine individuals (eight women; median age: 37.5 years; range: 32–62 years) during clinical remission. These individuals were under no treatment at the time of study. We obtained autopsied brain and spinal cord tissues from nine individuals who died with relapsing-remitting multiple sclerosis. We excluded the tissue from one individual because of unsuccessful immunohistochemistry, and analyzed tissue from eight individuals with relapsing-remitting multiple sclerosis (six brains and two spinal cord samples; three women; median age: 56.5 years; range: 40–67 years). We obtained the control brain from a subject with polymyositis.

Statistical analysis. Data are presented as means ± s.e.m. For EAE scores, significance among the groups was examined using Mann-Whitney *U* test. Other analyses were performed by one-way analysis of variance followed by Tukey's test or Student's *t* test. *P* values of <0.05 were considered significant.

Additional methods. Detailed methodology is supplied in the **Supplementary Methods**.

19. Polman, C.H. *et al.* Diagnostic criteria for multiple sclerosis: 2005 revisions to the "McDonald Criteria". *Ann. Neurol.* **58**, 840–846 (2005).

doi:10.1038/nm.2321

Supplementary Information Titles

Journal: Nature Medicine

Article Title:	**RGMa modulates T cell responses and is involved in autoimmune encephalomyelitis**
Corresponding Author:	Toshihide Yamashita

Supplementary Item & Number	**Title or Caption**
Supplementary Figure 1	Immunostaining for RGMa and neogenin in sections from MOG-EAE mice and individuals with MS.
Supplementary Figure 2	Distribution of RGMa-specific antibody in mice and knockdown of RGMa expressions.
Supplementary Figure 3	Determination of RGMa and neogenin expressions.
Supplementary Figure 4	Assessment of the *in vivo* mechanism of action of RGMa-specific antibody.
Supplementary Figure 5	T-cell responses to CD3-specific antibody in mice treated with RGMa-specific antibody or control IgG
Supplementary Methods	
Supplementary References	

RGMa modulates T cell responses and is involved in autoimmune encephalomyelitis

Rieko Muramatsu, Takekazu Kubo, Masahiro Mori, Yuka Nakamura, Yuki Fujita, Tsugio Akutsu, Tatsusada Okuno, Junko Taniguchi, Atsushi Kumanogoh, Mari Yoshida, Hideki Mochizuki, Satoshi Kuwabara and Toshihide Yamashita

Supplementary Information

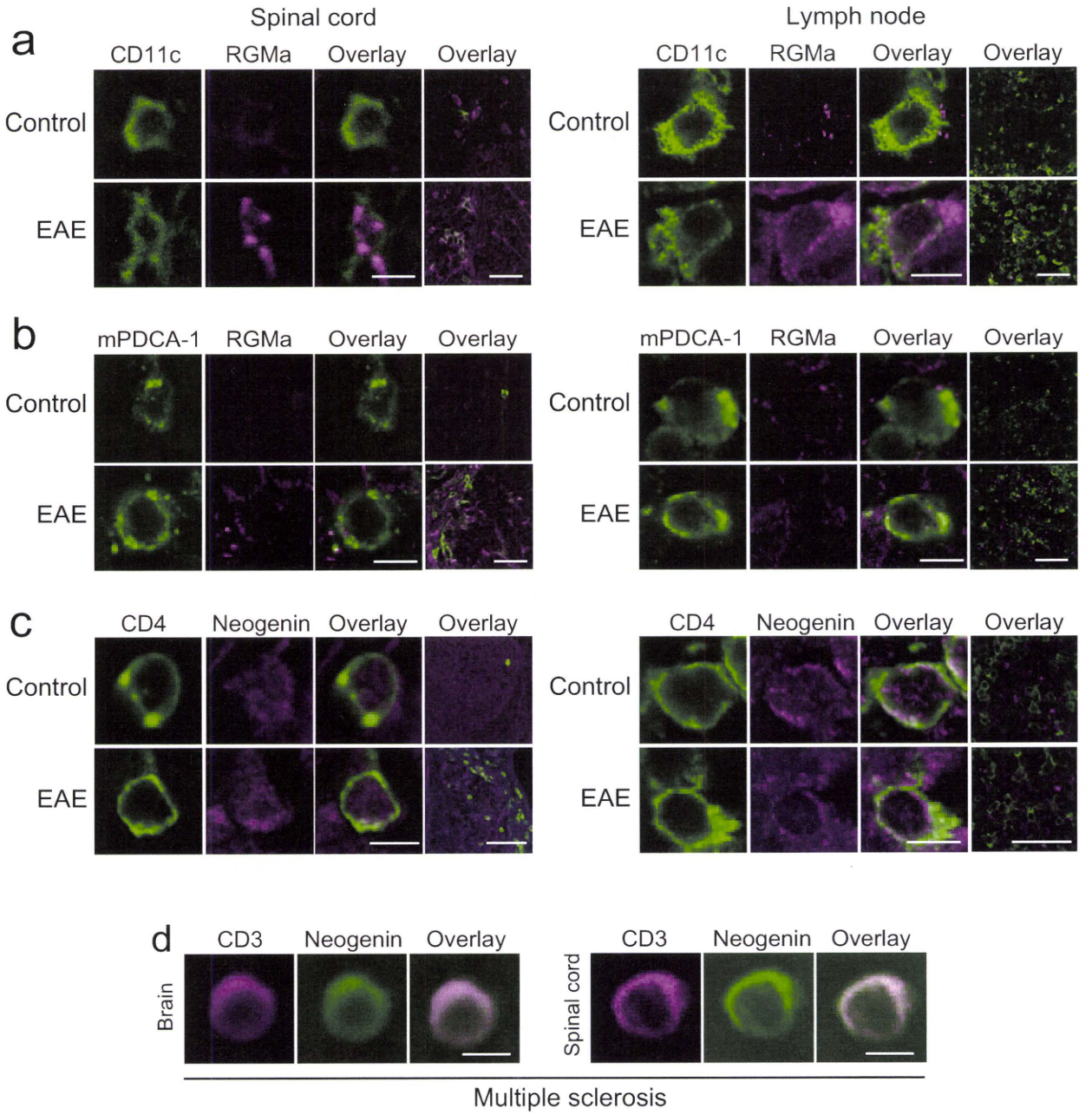

Supplementary Figure 1. Immunostaining for RGMa and neogenin in sections from MOG-EAE mice and individuals with MS. (a–c) Immunostaining for RGMa and neogenin expressions in combination with CD11c (a), mPDCA-1 (b), and CD4 (c) in lymph node and spinal cord sections from MOG-EAE and control mice. For details, please refer to Fig. 2a–c. Scale bar, 10 μm for high and 50 μm for low magnification images. **(d)** Double-labeling of brain and spinal cord sections with MS for neogenin and CD3. n = 8, scale bar = 5 μm.

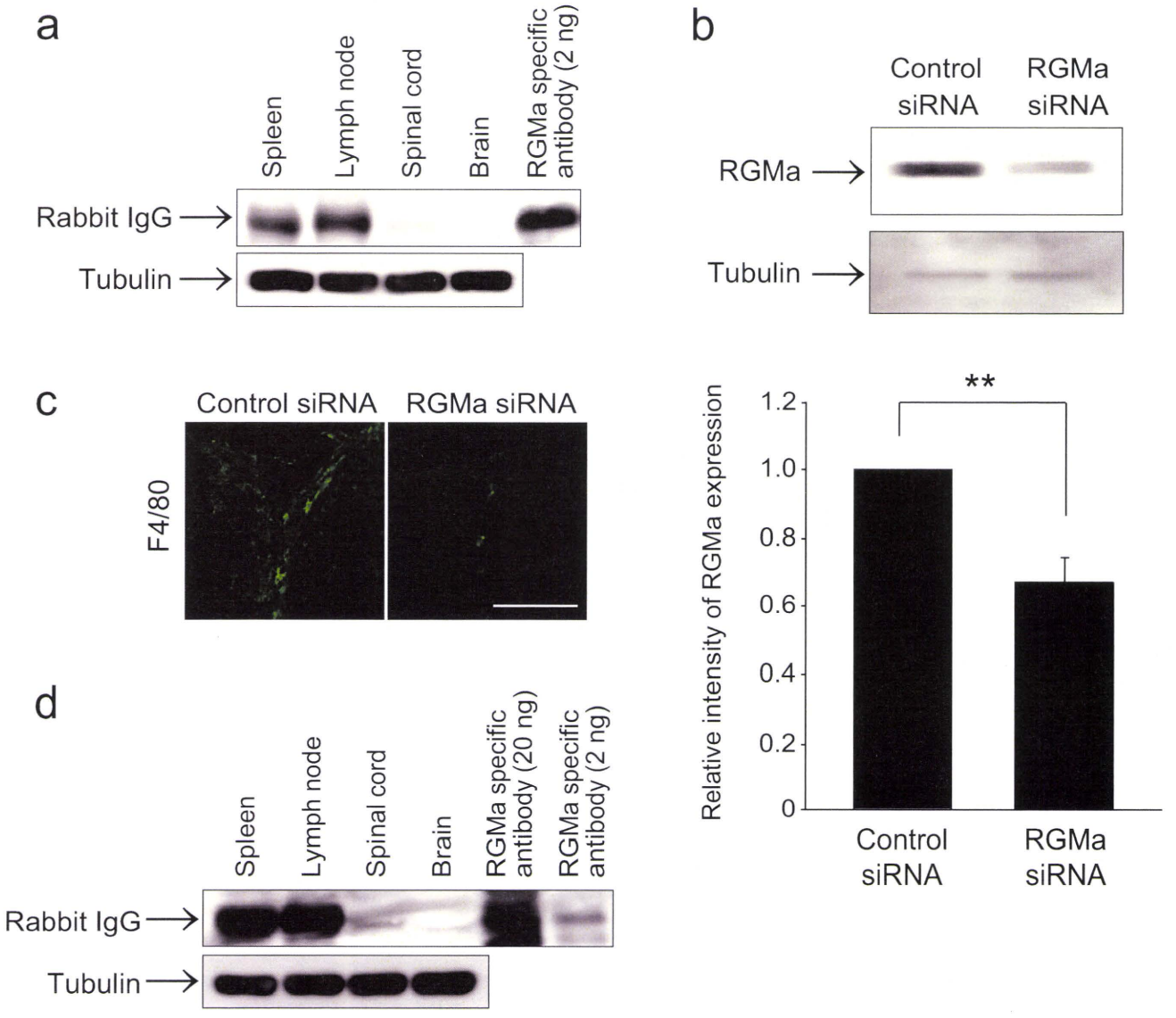

Supplementary Figure 2. Distribution of RGMa-specific antibody in mice and knockdown of RGMa expressions. (a) Western blots for detecting RGMa-specific antibody in several organs on d 7 after administration. **(b)** Western blots for detecting RGMa expression in RGMa siRNA-transfected BMDCs. The graph shows the relative expressions of RGMa. $^{**}P < 0.01$ by Student's *t*-test. **(c)** Representative images showing the presence of F4/80-positive cells in the spinal cord after the adoptive transfer of antigen-stimulated BMDCs with or without RGMa knockdown. The spinal sections were obtained at d 21 after EAE induction. Scale bar = 200 μm. **(d)** Western blots for detecting RGMa-specific antibody in several organs on d 11 after MOG immunization. RGMa-specific antibodies were administered by intraperitoneal injection to mice at d 7 and 10 after MOG immunization.

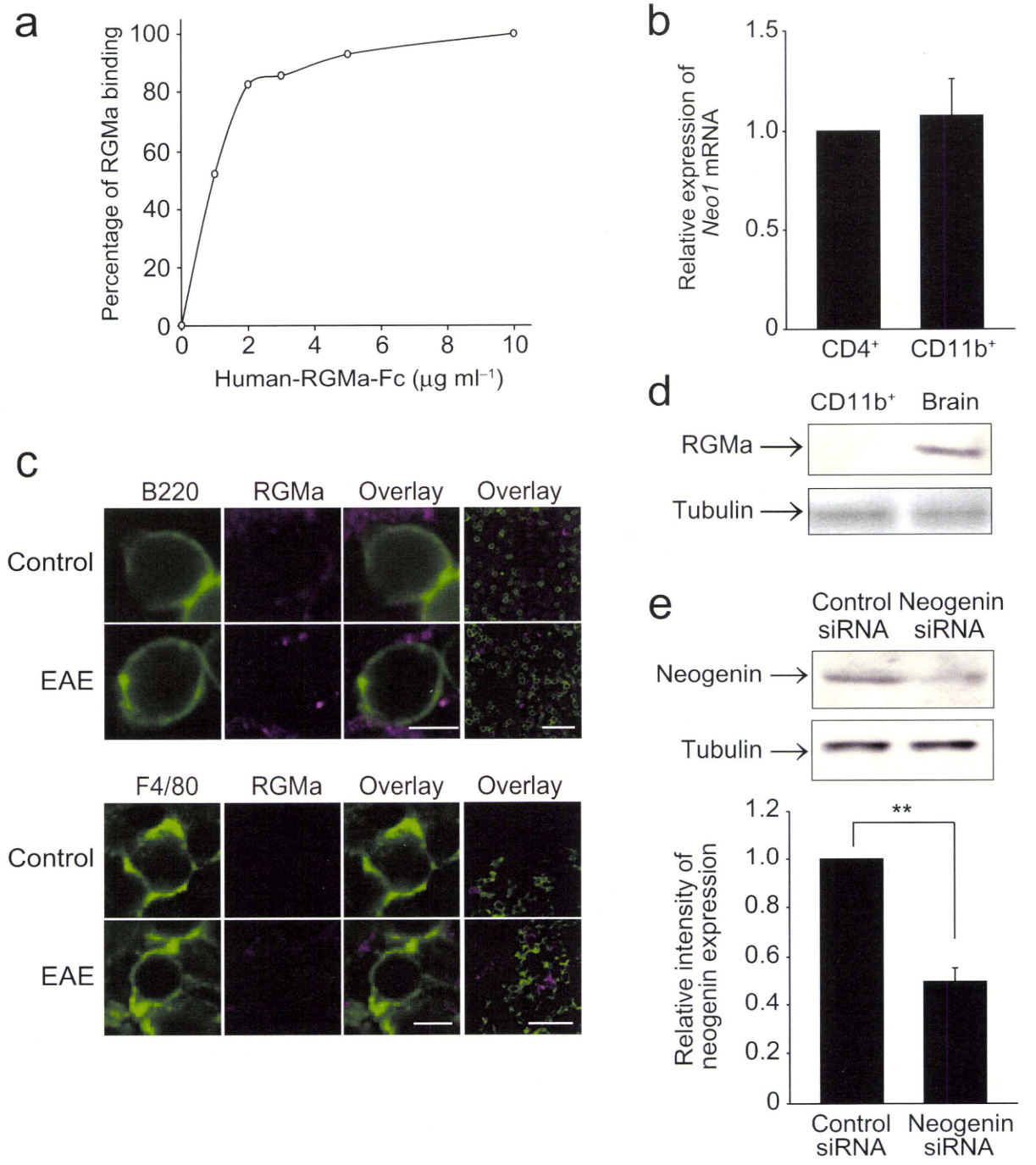

Supplementary Figure 3. Determination of RGMa and neogenin expressions. (a) Binding of human RGMa-Fc (indicated concentrations) to CD11b$^+$ cells in the spleen. **(b)** Relative expression of *Neo1* mRNA by RT-PCR analysis in CD4$^+$ T cells and CD11b$^+$ cells from the mouse spleen. The values represent the mean ± SEM of three independent experiments. **(c)** Immunostaining for RGMa in B220$^+$ cells or F4/80-positive macrophages from the spleen of MOG-EAE mice. Scale bar, 10 μm for high and 50 μm for low magnification images. **(d)** Western blots for RGMa expression in CD11b$^+$ macrophages isolated from the spleen of MOG-EAE mice and in the brain. **(e)** Western blots for detecting neogenin expression in neogenin siRNA-transfected BMMØs. The graph shows the relative expressions of neogenin. $^{**}P < 0.01$ by Student's *t*-test.

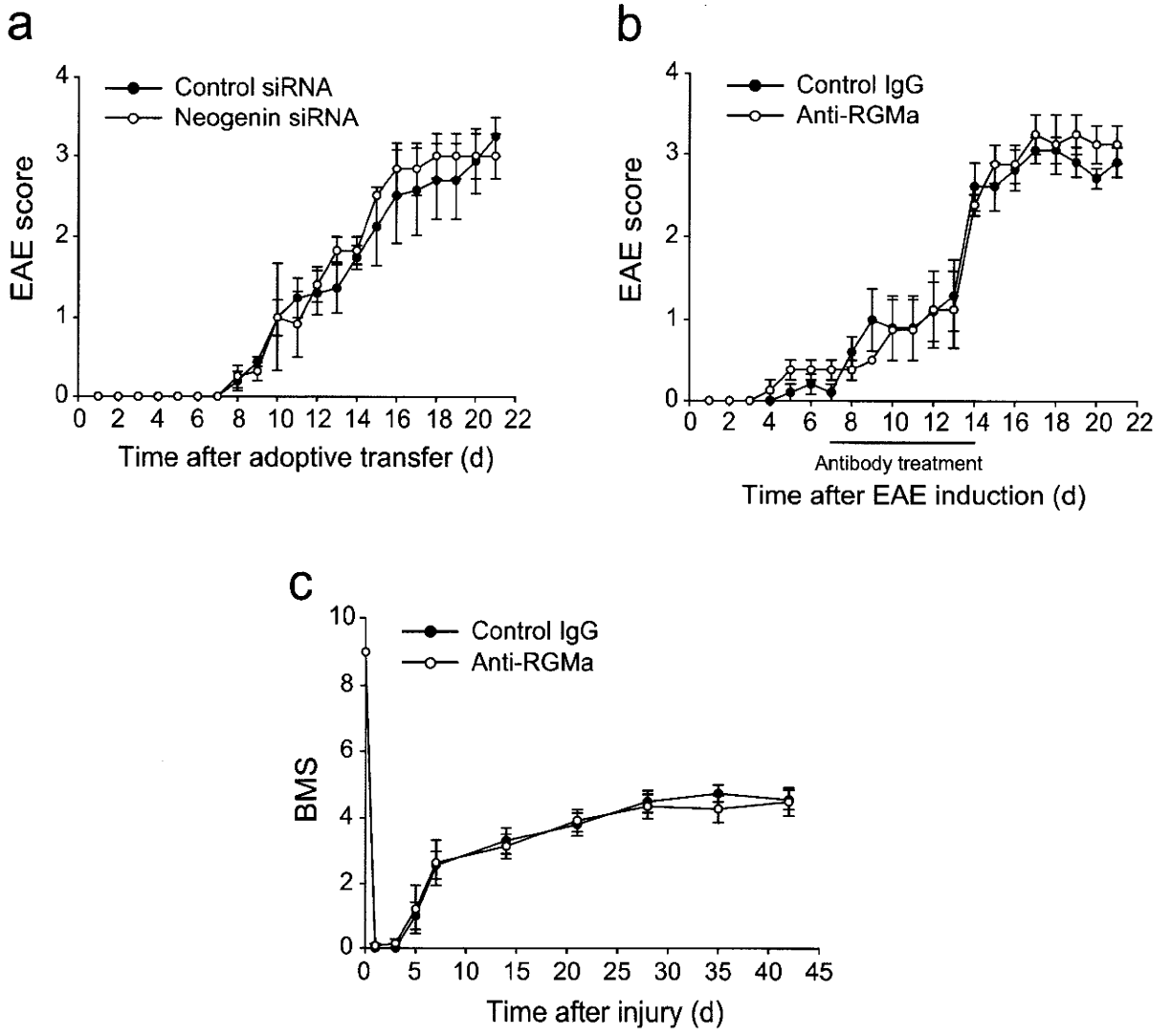

Supplementary Figure 4. Assessment of the *in vivo* mechanism of action of RGMa-specific antibody. (a) EAE scores in the CD11b-DTR mice that received adoptive transfer of macrophages with neogenin siRNA or control siRNA transfection (control siRNA, $n = 5$; neogenin siRNA, $n = 5$). **(b)** The progression of MOG-induced EAE in C57BL/6 mice after intrathecal administration of RGMa-specific antibody or control IgG in the cervical spinal cord (control IgG, $n = 4$; RGMa-specific antibody, $n = 5$). **(c)** BMS scores determined at the indicated time points after spinal cord contusion injury in mice intraperitoneally injected with control IgG or RGMa-specific antibody (control IgG, $n = 8$; RGMa-specific antibody, $n = 7$). All values represent the mean ± SEM (Mann–Whitney's *U* test).

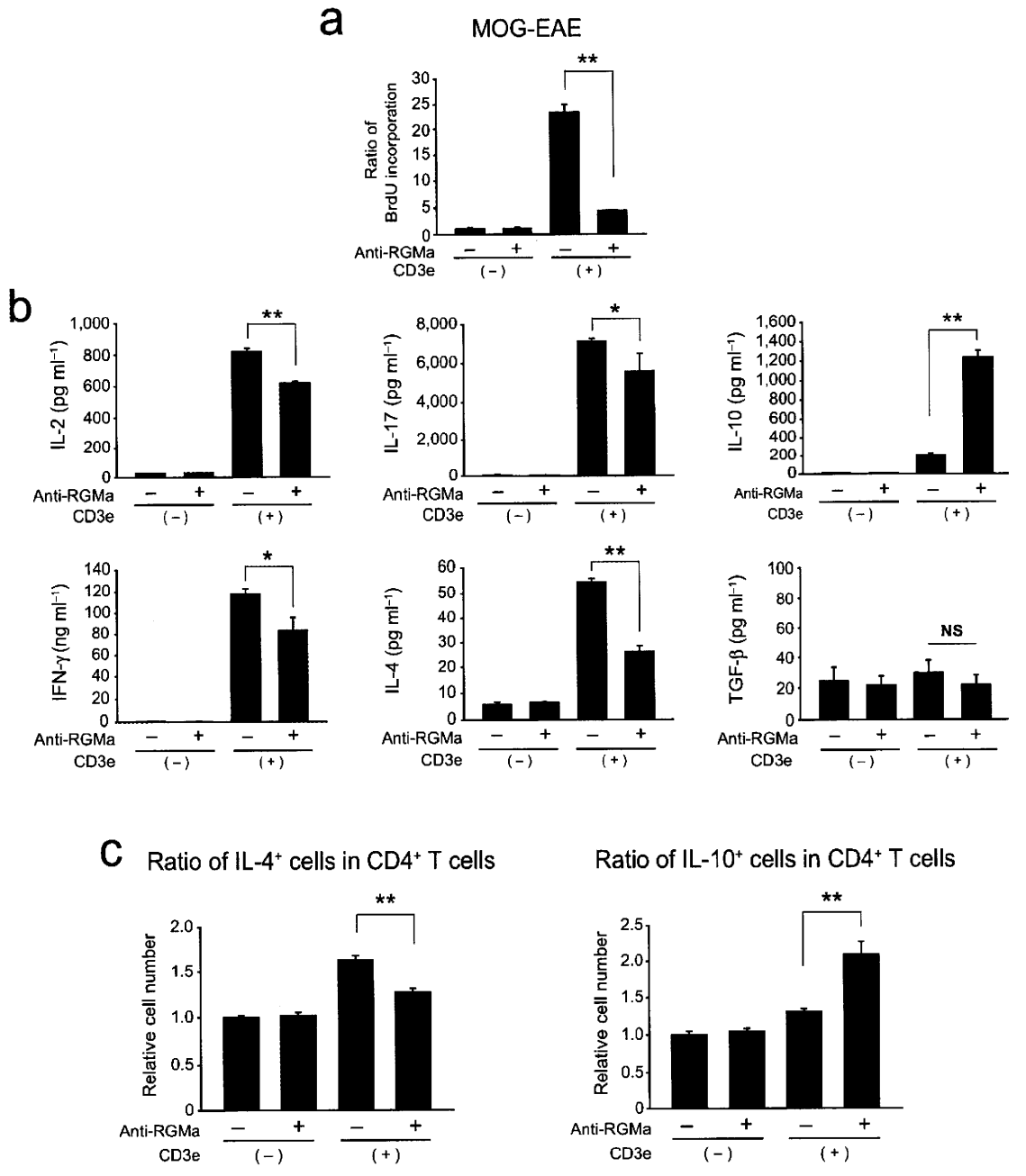

Supplementary Figure 5. T-cell responses to CD3-specific antibody in mice treated with RGMa-specific antibody or control IgG. (a) CD3-specific antibody-elicited proliferative responses in splenocytes obtained from mice treated with RGMa-specific antibody or control IgG on d 21 after the MOG immunization (control IgG, $n = 6$; RGMa-specific antibody, $n = 5$). **(b)** Production of IL-2, IL-4, IL-10, IFN-γ, TGF-β, and IL-17 by splenocytes obtained from mice treated with RGMa-specific antibody or control IgG (control IgG, $n = 6$; RGMa-specific antibody, $n = 5$). **(c)** The relative number of IL-4-producing T cells and IL-10-producing T cells with or without the RGMa-specific antibody treatment ($n = 3$ for each group). All values represent the mean ± SEM. $^{*}P < 0.05$, $^{**}P < 0.01$ by Student's *t*-test.

SUPPLEMENTARY METHODS

Cell preparation. We pressed freshly isolated spleens of C57BL/6 mice gently in RPMI-1640 medium (Invitrogen) and treated them with ACK lysing buffer (Lonza Walkersville) to remove erythrocytes. After washing thrice with RPMI-1640 medium, we filtered the cell suspension through a 70 μm cell strainer to obtain a single-cell suspension of splenocytes. We purified the $CD4^+$ T cells, $CD11b^+$ macrophages, and $CD45R^+$ B cells from the splenocytes by positive sorting, using CD4-, CD11b-, and CD45R-specific antibody-coated magnetic beads, respectively (Miltenyi Biotec). Further, we prepared BMDCs and BMMØs by culturing bone marrow cells with granulocyte-macrophage colony-stimulating factor (BMDCs) (20 ng ml^{-1}; Sigma-Aldrich) or macrophage colony-stimulating factor (BMMØ) (50 ng ml^{-1}; Sigma-Aldrich), respectively[21], and used these cells at 6 d after *in vitro* cultivation. For some of the experiments, we treated d 6 BMDCs with 0.01–1 μg ml^{-1} LPS (Sigma-Aldrich) for further activation.

Quantitation of mRNA expression. We isolated total RNA from the BMDCs by using an RNeasy kit (Qiagen), and obtained complementary deoxyribonucleic acid (cDNA) by using reverse transcriptase (RT; GE Healthcare). For quantitative analysis of RGMa mRNA expression (**Fig. 1a**), we used the cDNA as the template in a TaqMan real-time PCR assay (ABI Prism 7500 Sequence Detection System; Applied Biosystems), according to the manufacturer's protocol, and purchased specific primers and probes for the assay from Applied Biosystems. Further, we isolated total RNA from human PBMCs using Trizol (Invitrogen) and reverse-transcribed it by using a High-Capacity cDNA Reverse Transcription kit (Applied Biosystems). We examined the mRNA expression by real-time RT-PCR using

the TaqMan real-time PCR assay. We also employed TaqMan assays (Applied Biosystems) and a TaqMan Gene Expression Master Mix (Applied Biosystems) to quantify the gene expressions of IL-2 (Hs00914135_m1), IL-17a (Hs99999082_m1), IFN-γ (Hs99999041_m1), IL-4 (Hs00174122_m1), IL-10 (Hs00174086_m1), and TGF-β (Hs00998133_m1).

Next, we used SYBR Green assays to quantify mRNA expression for neogenin. We designed primers for neogenin by using Primer Express version 3.0 (Applied Biosystems), and determined the specificity of each primer set with a pretest showing the specific amplification for a specific gene by gel visualization and sequencing. We used a sample volume of 25 μl for the SYBR Green assays, which contained a 1× final concentration of Power SYBR Green PCR Master Mix (Applied Biosystems), 400 nM gene-specific primers, and 1 μl template. The PCR cycles started with an uracil-*N*-glycosylase digestion at 50°C for 2 min and an initial denaturation at 95°C for 10 min, followed by 40 cycles at 95 °C for 15 s, an annealing at 60°C for 1 min, and a gradual increase in temperature from 60 °C to 95 °C during dissociation stage. We normalized the relative mRNA expressions by measuring the amount of mRNA encoding glyceraldehyde 3-phosphate dehydrogenase in each sample, and calculated the cycle threshold values (Ct values) by using the ΔΔCt method to obtain the fold differences.

Western blotting. We lysed cells by using 2× sample buffer (250 mM Tris-HCl, 4% sodium dodecyl sulfate, 20% glycerol, 0.02% bromophenol blue, and 10% β-mercaptoethanol). After boiling for 5 min, we subjected equal volumes of the samples to 15% sodium dodecyl sulfate-polyacrylamide gel electrophoresis under reducing conditions and transferred the proteins to a polyvinylidene difluoride membrane (Immobilon-P; Millipore). After blocking it with phosphate-buffered saline (PBS) containing 5% skim milk and 0.05% Tween-20, we treated the membrane with RGMa-specific antibody[10]. For the detection, we used a horseradish peroxidase-conjugated secondary antibody (Cell Signaling Technology) and an

ECL chemiluminescence system (GE Healthcare). We quantified the protein expressions by using Scion Image software.

RGM-binding assay. We incubated splenocytes with different concentrations of human RGM-Fc for 30 min, washed and immunostained them with CD11b-specific PE-conjugated or CD4-specific APC-conjugated (BD Bioscience) antibody in combination with human Fc-specific FITC-conjugated antibodies (Sigma-Aldrich), and performed flow cytometric analysis. For analytical flow cytometry, we collected at least 10,000 events of lymphocytes on a BD Biosciences fluorescent-activated cell sorter (Calibur) and analyzed the data by using CellQuest software (BD Biosciences). We included the antibody isotype control for RGM-Fc staining and subtracted the level of background staining from the level of RGM-Fc staining.

Rap1 activity assay *in vitro* and *in vivo*. We measured Rap1 activity by using a Rap1 activation assay kit (Upstate Biotechnology). In brief, we treated $CD4^+$ T cells or splenocytes with or without 2 μg ml^{-1} of mouse recombinant RGMa (R&D Systems) for 5 min and lysed them in Mg^{2+} lysis buffer containing 25 mM *N*-2-hydroxyethylpiperazine-*N*′-2-ethanesulphonic acid (pH 7.5), 150 mM NaCl, 1% Igepal CA-630, 10 mM $MgCl_2$, 1 mM ethylenediaminetetraacetic acid, 2% glycerol, 2 mM sodium orthovanadate, 1 mM ethylsulfonyl fluoride, and protease inhibitor cocktails (Roche Diagnostics). We used cell lysates for estimating the total amount of Rap1. To precipitate active Rap1, we treated the cell lysates with the Ral-binding domain of the RalGDS–agarose conjugate for 30 min at 4 °C. We then washed the beads with the Mg^{2+} lysis buffer and resuspended them in 2× sample buffer for Western blotting using Rap1-specific antibodies (BD Bioscience) as described above.

We performed *in situ* detection of active Rap1 as described previously[22]. We fixed tissues in 4% paraformaldehyde (PFA) in 0.1 M phosphate buffer, incubated cryostat sections (10 μm) with blocking solution containing 5% bovine serum albumin (BSA) and 0.1% Triton X-100 in PBS for 1 h, and incubated them overnight at 4 °C in control glutathione S-transferase (GST) or GST-RalGDS (10 μg ml^{-1}). We washed the sections thrice, fixed them in 2% PFA in 0.1 M phosphate buffer for 10 min at room temperature, and washed them again. Then, we incubated them in GST-specific antibody (Santa Cruz Biotechnology) and CD4-specific antibody (BD Pharmingen) for 2 h at room temperature. We detected the signal by incubation with Alexa Fluor 488-conjugated antibody to mouse IgG and Alexa Fluor 546-conjugated antibody to rabbit IgG (Invitrogen) for 1 h at room temperature.

Lymphocyte-binding assay. We assessed cell adhesion as previously described[23,24]. In brief, flat-bottom Maxisorp 96-well plates (Nunc) were left uncoated (control) or precoated with 2 μg ml^{-1} recombinant mouse ICAM-1-Fc (for $CD4^+$ T cells; R&D Systems) overnight at 4 °C. We washed the plates with PBS and blocked the nonspecific binding sites with 2% BSA in RPMI-1640 medium (Invitrogen) for 1 h at 37 °C. We labeled purified $CD4^+$ T cells with 2.5 μM 2′,7′-bis-(2-carboxyethyl)-5-(and-6)-carboxyfluorescein acetoxymethyl ester (BCECF-AM; Calbiochem) for 30 min at 37 °C, followed by further washes with RPMI-1640 medium containing 0.5% BSA. We added a total of 5×10^5 cells to the precoated plates and incubated them for 1 h at 37 °C in 0.5% BSA–RPMI-1640 with or without 2 μg ml^{-1} recombinant RGMa. Where indicated, we pretreated $CD4^+$ cells with 20 μM of GGTI-298 (Calbiochem) for 1 h. We removed the nonadherent cells by washing the culture thrice with warm 0.5% BSA–RPMI-1640. We quantified adhesion by using SpectraMAX (Molecular Devices) at an excitation wavelength of 485 nm and emission wavelength of 538 nm. We quantified specific adhesion by subtracting the total number of fluorescent-positive cells in

the untreated wells. The adhesion was expressed as a ratio of specific cell attachment divided by the total input cell number.

In another experiment (**Fig. 4d**), we immunized mice with myelin oligodendrocyte glycoprotein (MOG) and complete Freund's adjuvant. At d 21 after the induction of EAE, we labeled freshly isolated $CD4^+$ T cells with BCECF-AM and incubated the cells with or without RGMa-specific antibody. We then calculated the ratio of specific cell attachment.

Immunohistochemical staining of mouse tissues. After 1, 2, and 3 weeks from EAE induction, we perfused mice transcardially with 4% PFA in PBS. We postfixed their spleen, lymph node, spinal cord, and brain tissues in the same fixatives at 4 °C overnight; soaked them in 30% sucrose and PBS; and then embedded them in optimal cutting temperature compound. We cut frozen cross-sections at 5 or 10 μm with a cryostat and mounted them on Matsunami adhesive silane-coated slides. We permeabilized the sections in PBS containing 0.1% Triton-X100, 10% goat serum, and 1% BSA for 1 h at room temperature and then incubated them with primary antibodies overnight at 4°C, followed by incubation with fluorescence-conjugated secondary antibodies for 1 h at room temperature. We used the following primary antibodies: RGMa-specific rabbit (IBL), neogenin-specific rabbit (Santa Cruz Biotech), CD11b-specific rat (Serotec), CD4-specific rat (BD Bioscience), mPDCA-1-specific rat (Miltenyi Biotec), CD11c-specific hamster (BD Bioscience), B220-specific rat (BD Bioscience), APP-specific rabbit (Invitrogen), and F4/80-specific rat (Serotec) antibodies. We used Alexa Fluor 488- or 568-conjugated goat antibody to rabbit IgG, goat antibody to rat IgG, and goat antibody to hamster IgG (Invitrogen) as the secondary antibodies. For quantification of the immunofluorescence intensities in each cell, we traced the contour of the cell manually on a counterstained image of the corresponding cell-type marker. We determined the fluorescence intensities for RGMa or neogenin within the contour

of the cell. We determined the background fluorescence of the cells by performing an identical analysis with cells labeled in the absence of the primary antibodies. We then averaged the values of the background fluorescence intensity from twenty cells and subtracted these values from the signals obtained by the immunofluorescent staining[25]. We determined the average intensities for 50–100 cells from each animal and normalized the relative intensities by using those of the controls.

To assess demyelination in the spinal cord, we performed myelin staining by using a green fluorescent lipophilic dye (FluoroMyelin, Invitrogen) according to the manufacturer's instructions; we also double-labeled the section with 4′,6-diamidino-2-phenylindole (DAPI). We identified demyelinating lesions in the ventral white matter as regions without FluoroMyelin staining.

Immunohistochemical staining of human tissues and PBMCs. We obtained tissue samples and PBMCs of individuals with MS from Chiba University, Kitasato University, and Aichi Medical University. We fixed the brain and spinal cord samples in formalin, embedded them in paraffin, and cut them in 4-μm-thick sections for immunohistochemistry. We then deparaffinized, washed, and subjected the sections to an antigen-retrieval procedure. We incubated tissue samples with human CD83-specific mouse (Serotec) or human CD209-specific (BD Pharmingen) antibodies together with human RGMa-specific antibodies (R&D System). In another experiment, we incubated the tissue samples with human CD3-specific antibody (Dako) and human neogenin-specific antibody (Santa Cruz Biotechnology). We used Alexa Fluor 488- or 568-conjugated goat anti-mouse IgG and goat anti-rat IgG (Invitrogen) as the secondary antibodies.

We sedimented the PBMCs on polyethylenimine-coated glass slides. For staining, we fixed the cells in 4% PFA in PBS and incubated them with human CD3-specific antibody and